NUCLEIC ACID THERAPEUTICS
Volume 00, Number 0, 2015

DOI: 10.1089/nat.2014.0505

Original Article

siRNA Delivery to the Glomerular Mesangium Using Polycationic Cyclodextrin Nanoparticles Containing siRNA

Jonathan E. Zuckerman,[1] Aaron Gale,[1] Peiwen Wu,[2] Rong Ma,[2] and Mark E. Davis[1]

There is an urgent need for new therapies that can halt or reverse the course of chronic kidney disease with minimal side-effect burden on the patient. Small interfering RNA (siRNA) nanoparticles are new therapeutic entities in clinical development that could be useful for chronic kidney disease treatment because they combine the tissue-specific targeting properties of nanoparticles with the gene-specific silencing effects of siRNA. Recent reports have emerged demonstrating that the kidney, specifically the glomerulus, is a readily accessible site for nanoparticle targeting. Here, we explore the hypothesis that intravenously administered polycationic cyclodextrin nanoparticles containing siRNA (siRNA/CDP-NPs) can be used for delivery of siRNA to the glomerular mesangium. We demonstrate that siRNA/CDP-NPs localize to the glomerular mesangium with limited deposition in other areas of the kidney after intravenous injection. Additionally, we report that both mouse and human mesangial cells rapidly internalize siRNA/CDP-NPs in vitro and that nanoparticle uptake can be enhanced by attaching the targeting ligands mannose or transferrin to the nanoparticle surface. Lastly, we show knockdown of mesangial enhanced green fluorescent protein expression in a reporter mouse strain following iv treatment with siRNA/CDP-NPs. Altogether, these data demonstrate the feasibility of mesangial targeting using intravenously administered siRNA/CDP-NPs.

Introduction

CHRONIC KIDNEY DISEASE (CKD) is a widespread medical condition that for many patients will inevitably progresses toward end stage renal disease despite medical intervention [1]. Even with its often unrelenting course, CKD is relatively asymptomatic for the afflicted patient who must endure lifelong treatment with tangible side effects. There is an urgent need for new therapies that can stop or reverse the course of chronic kidney disease with minimal side-effect burden on the patient. Small interfering RNA (siRNA) nanoparticles are novel therapeutic entities in clinical development that could be useful for this indication. siRNA nanoparticles combine the tissue specificity characteristic of nanoparticle therapeutics [2] with gene-specific silencing effects of siRNA [3]. This rational combination of therapeutic modalities is a promising strategy for diseases, such as CKD, that would benefit from highly specific tissue targeting with minimal off-target effects.

Several reports have highlighted the kidney glomerulus as an accessible target for nanoparticle based therapeutics [4]. Choi et al., have demonstrated that intravenously (i.v.) administered PEGylated gold nanoparticles (under 100nm) have a restricted kidney deposition within the mesangium [5]. Liao et al. showed that i.v. TRX-20-prednisolone loaded liposome treatments reduced glomerular mesangial immunoglobin A (IgA) and C3 depositions in a mouse model of IgA nephritis (ddY mice) [6]. Morimoto et al. reported that a single i.v. injection of TRX-20-prednisolone loaded liposomes given to a rat model of human mesangial proliferative glomerulonephritis (anti-Thy-1 nephritis model) reduced the total glomerular cell number and level of α-smooth muscle actin–positive cells at a markedly reduced dose compared with daily injections of a prednisolone saline solution [7]. Kamps et al. demonstrated that i.v. doses of dexamethasone-containing monoclonal anti-E-selectin antibody-targeted immunoliposomes (Dexa-Ab_{Esel} liposomes) decreased plasma blood urea nitrogen levels, glomerular proinflammatory gene levels, and the percentage of crescent glomeruli in an anti-glomerular basement membrane glomerulonephritis mouse model. Notably, Dexa-Ab_{Esel} liposome treatment did not result in elevation of plasma glucose levels, as was observed with administration of free dexamethasone [8]. Suana et al. showed that single i.v. administration of low dose mycophenolate mofetil-OX7-immunoliposomes (MMF-OX7-ILs) resulted in less severe nephritis, with decreased mesangial expansion, compared with free MMF in rat anti-thymocyte antigen 1 (Thy1.1) nephritis [9]. Importantly, liposomal delivery of MMF required only half the standard total MMF dose to achieve these therapeutic effects.

[1]Chemical Engineering, California Institute of Technology, Pasadena, California.
[2]Department of Integrative Physiology and Cardiovascular Research Institute, University of North Texas Health Science Center, Fort Worth, Texas.

Altogether, these literature examples demonstrate feasibility of nanoparticle therapeutic delivery to the glomerulus with reduced off-target effects and toxicities.

Only two reports of systemically administered siRNA delivery to the glomerulus have been reported. Shimizu et al. have reported "proof of principle" results showing that a siRNA/cationic polymer (PLLg) delivery system can reach the glomerulus following intraperitoneal administration [10]. Administration of these nanocarriers to lpr mice (mouse lupus nephritis model) resulted in the decrease of MAPK1 expression and reduced sclerosis within the nephritic glomeruli of these mice. Hauser et al. have demonstrated that coupling of siRNA to an antibody can be used for specific siRNA delivery to podocytes following i.v. administration [11].

We have previously reported that cyclodextrin-containing siRNA nanoparticles (siRNA/CDP-NPs) quickly accumulate in the glomerular basement membrane after i.v. administration [12]. This nanoparticle formulation (Fig. 1) of siRNA (not chemically modified) with a cationic, cyclodextrin-containing polymer (CDP)-based delivery vehicle (clinical version denoted CALAA-01) has been shown to accumulate in human tumors and deliver functional siRNA from a systemic, i.v. infusion [13]. Given its glomerular localization and its clinical utility, we decided to explore the potential of this siRNA/CDP-NP for siRNA delivery to the mesangium. Here, we test the hypothesis that the siRNA/CDP-NPs can deliver siRNA to the glomerular mesangium to facilitate the knockdown of target genes in this tissue compartment.

Materials and Methods

Small interfering RNA/CDP nanoparticle formulation

siRNA nanoparticles were formed by using cyclodextrin-containing polycations (CDP), adamantane-polyethylene glycol (AD-PEG), AD-PEG-mannose, and AD-PEG-transferrin as previously described (precomplexation) [14]. Nanoparticles were formed in 5% glucose in deionized water at a charge ratio of 3 +/− and a siRNA concentration of 2 mg/mL unless otherwise indicated. Twenty-one base pair unmodified and cyanine 3 (Cy3)-labeled oligos were purchased from Qiagen. Sense strand sequences are as follows: siRNA targeting enhanced green fluorescent protein (EGFP) (5′-GGCUACG UCCAGGAGCGCACC-3′) from Novina et al. (2002) [15], control siRNA (siCON) (5′-UAGCGACUAAACACAUCAA UU-3′), siTRACE (5′-CCUGCGAACACACAAGCUCCU-3′). siRNA/CDP nanoparticles formulated with 80 mole percent Cy3-siGL3 and Alexa Fluor 350 (AF350)-CDP were similar in size and stability to their nonlabeled counterparts (Supplementary Fig. S1; Supplementary Data are available online at www.liebertpub.com/nat).

Synthesis of AF350-labeled CDP

CDP (30 mg) and Alexa Fluor® 350 succinimidyl ester (5 mg, Invitrogen) were transferred to a flask wrapped in aluminum foil and dried under vacuum for 2 hours; 0.5 mL of anhydrous dimethyl sulfoxide and N,N-diisopropylethylamine (0.7 μL) were subsequently added under argon. The reaction was allowed to proceed in the dark under argon with constant stirring overnight. The reaction mixture was dialyzed against water three times via a 3-kDa membrane centrifuge filter device (Amicon). The retentate was then filtered through a 0.2 μm filter (Palls) and lyophilized to yield a yellow colored product.

Synthesis of AD-PEG-mannose

Three one hundredths millimoles of H-hydroxysuccinimide-PEG-maleimide was added to 0.18 mmol of 4-aminophenyl alpha-D-mannopyranoside in phosphate-buffered saline (PBS), pH 7.5, and incubated for 1 hour at room temperature. Reaction mixture was then dialyzed against water, 0.1μm, and lyophilized. One hundred nine milliggrams of mannose-PEG-maleimide and 13.3 mg of admantane-SH were dried under vacuum for 1 hour; 2 mL of anhydrous dimethyl sulfoxide was then added under inert gas and reaction was incubated overnight at room temperature. Water was added and insoluble material was removed by centrifugation. The supernatant was dialyzed against water and 0.2 μm filtered and purified over 2× TSKgel G3000SWxl columns with PBS pH 7.2 at 0.5 mL/minute as the eluent. The appropriate fraction was collected and lyophilized. Structure was verified by proton nuclear magnetic resonance and matrix assisted laser desorption ionization time-of-flight (Supplementary Fig. S2).

Cell culture

SV40-MES (mouse mesangial) and CRL-2573 (rat mesangial) cells were obtained from ATCC. Human mesangial cells were obtained from ScienCell. For siRNA/CDP NP uptake experiments, cells seeded in six-well plates were washed

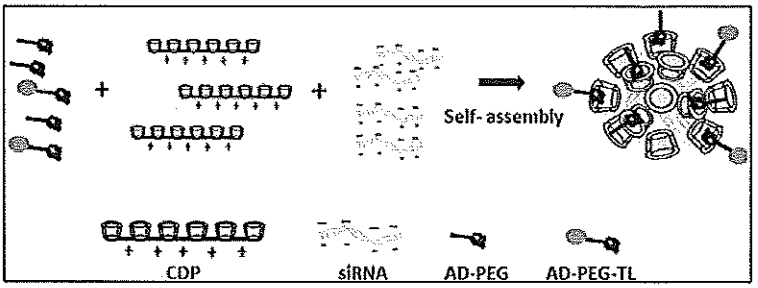

FIG. 1. Schematic of small interfering RNA/cyclodextrin-containing polymer nanoparticle (siRNA/CDP-NP) assembly. When mixed together in aqueous solution (5% dextrose), the cationic CDPs assemble with the negatively charged siRNA molecules via electrostatic interaction. Five-kilodalton polyethylene glycol (PEG) molecules are covalently linked to the small molecule adamantane (AD) and will form guest/host interactions with the cyclodextrin component of the nanoparticle thereby providing satiric stabilization to the nanoparticles. The distal end of the AD-PEG molecules can be covalently linked to targeting ligands (TL) such as mannose or transferrin that facilitate cellular internalization of the nanoparticles.

with PBS and siRNA/CDP NPs suspended in 2 mL of opti-MEM (Invitrogen) were applied. Total siRNA concentration was 100 nM. At the indicated time points the nanoparticle solution was removed and the cells washed with cell scrub buffer (Gene Therapy Systems) to remove surface associated nanoparticles or nucleic acids prior to analysis. Cells were imaged directly in the six-well plates for the epifluorescence experiments. Cells were trypsinized in 1× trypsin (Invitrogen), washed, and resuspended in PBS for flow cytometry experiments, which were performed on a FACSCalibur (BD Biosciences) flow cytometer and data analysis was performed using Flowing Software version 2.5.1.

Animal studies

This study was carried out in strict accordance with the recommendations in the Guide for the Care and Use of Laboratory Animals of the National Institutes of Health. The protocol was approved by the Caltech Institutional Animal Care and Use Committee (Protocol 1502). Si-6 to nine-week-old, female Balb/c mice and C57BL/6-Tg(CAG-EGFP)1Osb/J (Stock No. 003291) mice were obtained for the Jackson Laboratory. Mice were euthanized by carbon dioxide overdose for organ collection at indicated time points. All organs were fixed in 4% (w/v) paraformaldehyde in PBS overnight. For confocal imaging, siRNA/CDP NP formulations contain 80 mole percent Cy3-siTRACE and AF350-CDP were administered via i.v. tail vein injections at a dose of 5 or 10 mg/kg siRNA in ~100 μL injection volume. Formalin-fixed organs were dehydrated and embedded in molten paraffin to generate sections 4 μm in thickness.

In vivo EGFP knockdown experiment

Mice received i.v. doses of transferrin-targeted siRNA/CDP NPs containing control siRNA (siCON), transferrin-targeted siRNA/CDP NPs containing siEGFP, or mannose-targeted siRNA/CDP NPs containing siEGFP at a dose of 10 mg/kg siRNA on day 1 and 3 of the experiment. Mice were killed on day 5 for kidney harvesting and tissue processing. Slides were imaged in a blinded fashion with fixed detector gain; 70–72 consecutively identified glomeruli from each slide were imaged. Data sets were scored prior to unblinding.

Transmission electron microcopy

Tissue blocks (~1 mm^3) were fixed in 2.5% glutaraldehyde (in 0.1 M sodium cacodylate, pH=7.4) for 2 hours, stained by 1% OsO_4 at 4°C for 2 hours, and 0.9% osmium tetroxide (OsO_4) and 0.3% potassium ferrocyanide at 4°C for 2 hours. Gradual dehydration with ethanol and propylene oxide enabled tissue embedding in Epon 812 resins (Electron Microscopy Sciences); 80-nm-thick sections were deposited on carbon and formvar-coated, 200-mesh, nickel grids and stained with 3% uranyl acetate and Reynolds lead citrate for visualization under a 300 kV TF30UT transmission electron microscope.

Fluorescent microscopy

Sections were deparrafinized with xylene, rehydrated, and mounted with ProLong Gold antifade reagent (Invitrogen) for viewing.

Confocal microscopy

Images were obtained on a Zeiss LSM 510 inverted confocal scanning microscope (with a Zeiss PlanApochormat× 63/1.4 oil objective). The anti-CD90/Thy1 (MRC OX-7) mouse monoclonal antibody (Abcam: ab225) was used at 1:100 dilution. The excitation wavelength for AF350-CDP and 4',6-diamidino-2-phenylindole was 705 nm (two-photon laser) and 543 nm (helium–neon laser) for Cy3-siRNA. Their corresponding emission filters were 390–465 nm, and 565–615 nm respectively. The measured resolution at which images were acquired is 512×512 pixels, and the image bit-depth is 8 bits. The Zeiss LSM Image Browser Software allows the extraction of images.

Epifluorescent microscopy

Images were obtained on an Olympus IX50 fluorescent microscope (with an Olympus UPlanfluor 40×/1.3 oil objective).

Magnetic bead based glomerular isolation

Glomeruli were isolated using the method developed by Takemoto et al. [16]. Briefly, mice were perfused with Dynabeads (M-450 tosylactivated) (Invitrogen) suspended in PBS immediately post mortem via infusion through the left ventricle. Kidneys were subsequently minced with a razor blade followed by digestion with collagenase and DNaseI for 1 hour at 37°C. Digested material was passed through two 5 μm cell strainers (BD bioscience) and pooled with subsequent PBS washes of the strainers. Material was pelleted at 200 g for 10 minutes. The supernatant was decanted and the pellet resuspended in PBS. The tube containing the resuspended pellet was placed on the magnet (Invitrogen) and the magnet bound material was washed three times with PBS. Magnet bound material was resuspended in PBS and confirmed to contain glomeruli via light microscopy.

RNA isolation and real time reverse transcription polymerase chain reaction

Total RNA was isolated from cells using the miRNeasy kit (Qiagen) following manufacturer's instructions and quantified using a Nanodrop 2000 spectrophotometer (Thermo). Custom Taqman microRNA quantitative polymerase chain reaction (PCR) assays (Applied Biosystems) for siTrace were used for quantification of siRNA from total RNA. Reverse transcription and PCR reactions were performed as described in the product manual. Real-time PCR analysis was performed using a MyiQ Single Color Real Time PCR Detection System (Bio-Rad).

Results

Rapid siRNA nanoparticle internalization observed for mouse and human mesnagial cells in vitro

To demonstrate the feasibility that human and mouse mesangial cells will internalize siRNA/CDP-NPs, we examined the uptake of siRNA/CDP-NPs by mesangial cells in vitro using Cy3-siRNA containing siRNA/CDP-NP formulations. Cy3-siRNA fluorescence intensity was measured via both epifluorescence microscopy and flow cytometry. Both mouse and human mesangial cells internalized the

siRNA/CDP-NPs, but not free siRNA, after only 5 minutes of exposure (Fig. 2A; Supplementary Fig. S3A, B). We confirmed these observations via flow cytomerty (Fig 2B). We also observed siRNA/CDP-NP uptake in rat mesangial cells (Supplementary Fig. S3C).

Intravenously administered siRNA/CDP nanoparticles deposit within the mouse kidney mesangium

To determine whether i.v. administered siRNA/CDP-NPs deposit in the mesangium, we interrogated the level of fluorescent signal present in fixed sections of kidney tissue from mice that received i.v. siRNA/CDP-NPs that contain fluorescent components (Cy3-labed siRNA and AF350-labeled CDP). Fluorescent signal in the kidney after i.v. administration of free Cy3-siRNA was found within tubule cells at 10 minutes after injection and was nearly undetectable 120 minutes after injection (Fig. 3A). No detectable fluorescence signal was observed in the glomeruli of these mice. However, following i.v. administration of Cy3-siRNA/CDP-NPs the opposite phenomenon was observed. Strong Cy3-siRNA fluorescence signal was detected within all glomeruli examined at 10 minutes post injection, with minimal signal in tubule cells (Fig. 3A). Although greatly attenuated, Cy3-siRNA fluorescent signal was still clearly detectable in glomeruli 120 minutes after i.v. administration with minimal accumulation in other kidney compartments. We also observed some fluorescent signal in the peritubule interstitial space following siRNA/CDP-NP administration, but not free siRNA administration (Supplementary Fig. S4).

To determine whether these siRNA/CDP-NP formulations were depositing as intact nanoparticles in the glomerulus, we examined the glomerular fluorescent signal from mice receiving siRNA/CDP-NP formulations containing both Cy3-siRNA and AF350-CDP (Fig. 3B). Strong AF350-CDP fluorescence that colocalized with the Cy3-siRNA signal was observed in glomeruli at 10 minutes after injection. Although greatly attenuated, colocalized glomerular Cy3-siRNA and AF350-CDP fluorescence was still detected in all glomeruli at 120 minutes post dose. We confirmed these observations by transmission electron microscopy analyses that revealed electron dense objects in the glomerular capillary wall consistent in size and shape with intact siRNA/CDP-NPs (Fig. 3C).

To confirm delivery of siRNA/CDP-NPs to the mesangium, we counter-stained tissue sections from mice that received Cy3-siRNA containing nanoparticles with the mesangial marker thymic antigen 1 (Thy1) using the OX-7 monoclonal antibody (Fig. 3D). We found persistent Cy3-siRNA fluorescent signal 48 hours after administration of the siRNA/CDP-NPs that colocalized with the OX-7 antibody staining. Semiquantitative colocalization analysis of Cy3-siRNA fluorescence and OX-7 staining using BioImageXD software revealed 88% OX7 staining colocalization with Cy3-fluorescnece and 91% colocalization of Cy3-siRNA fluorescence with OX-7 staining. These data suggest that siRNA/CDP-NP deposition in the glomerulus is primarily mesangial.

Outside the kidney, siRNA/CDP-NPs have restricted distribution to liver sinusoids, and splenic red pulp

The restricted biodistribution of nanoparticle therapeutics is paramount in limiting their off-target toxicities. Therefore,

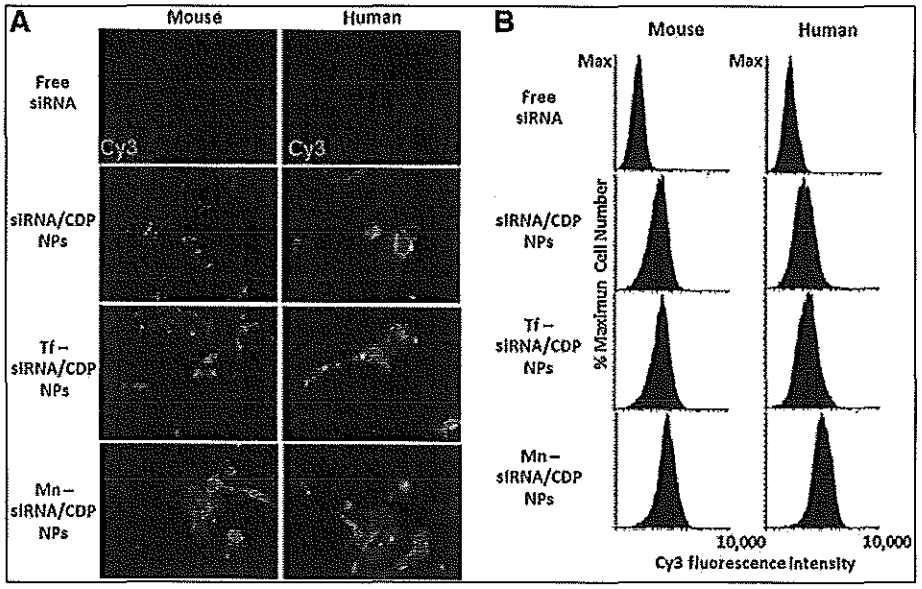

FIG. 2. In vitro uptake of siRNA/CDP-NPs by mouse and human mesangial cells and modulation of uptake with targeting ligands. Analysis of in vitro uptake of cyanine 3 (Cy3)-siRNA labeled siRNA/CDP-NPs by mouse or human mesangial cells. **(A)** Epifluorescence microscopy images of mesangial cells following a 5-minute exposure to siRNA/CDP-NPs. **(B)** Flow cytometry analysis of Cy3-siRNA fluorescence intensity in mesangial cells following exposure to siRNA/CDP-NPs for the indicated amount of time. Detector gain and exposure time for all epifluorescence images was fixed for each experiment. Global brightness and contrast were adjusted across whole images to improve clarity of images on scale for publication. Color images available online at www.liebertpub.com/nat

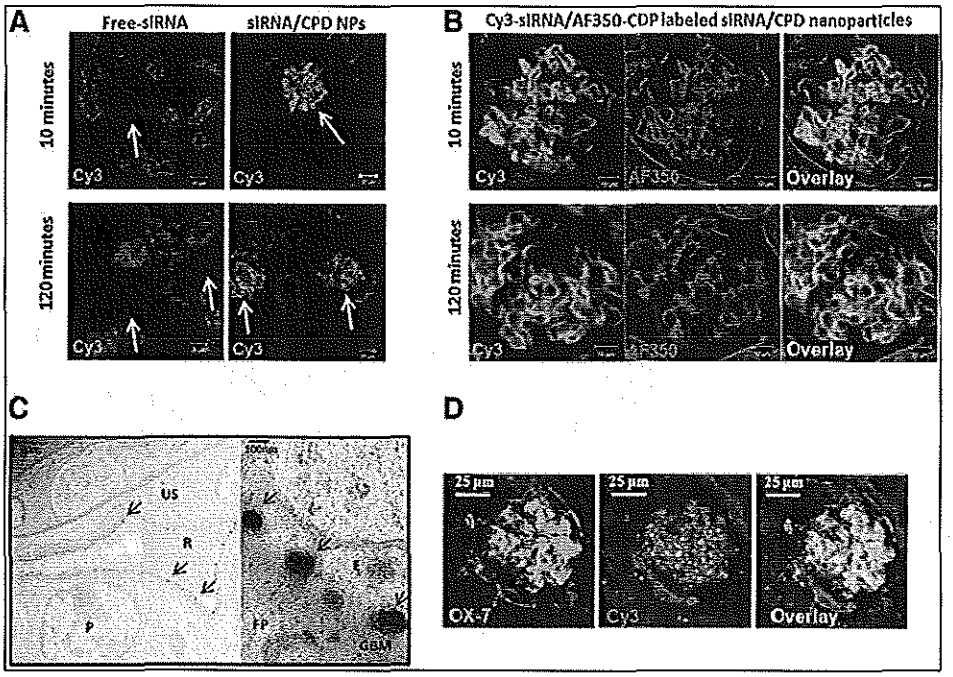

FIG. 3. siRNA/CDP-NPs accumulate in mouse glomeruli following intravenous (i.v.) administration. **(A)** Laser scanning confocal microcopy of kidney sections from mice that received iv doses of free Cy3-siRNA or Cy3-siRNA labeled siRNA/CDP-NPs. Solid arrows point to glomeruli. **(B)** High magnification images of glomeruli from mice that received iv doses siRNA/CDP-NPs dual labeled with Cy3-siRNA/AF350-CDP fluorescent labels. **(C)** Transmission electron microscopy images from the glomerulus of a mouse 10 minutes following an iv dose of siRNA/CDP-NPs. Black arrows point to spherical electron dense deposits that are consistent in size with siRNA/CDP-NPs. BM, glomerular basement membrane; E, endothelial cell; FP, podocyte foot process; P, podocyte; R, red blood cell; US, urinary space. **(D)** Fluorescence microscopy image of a mouse glomerulus 48 hours after administration of Cy3-siRNA labeled siRNA/CDP-NPs. Tissue section were costained for thymic antigen 1 (Thy1) mesangial marker with the OX-7 monoclonal antibody. For all images, the detector was adjusted for maximal dynamic range or until diffuse background autofluorescence in proximal tubules was apparent. Global brightness and contrast were adjusted across whole images to improve clarity of images on scale for publication. Color images available online at www.liebertpub.com/nat

we explored the deposition of the Cy3-siRNA/CDP-NPs in other organs (Fig. 4). Bright and diffuse Cy3-siRNA fluorescent signal was observed in liver and spleen, whereas only focal areas of fluorescent signal nearly indistinguishable from tissue background autofluorescence were observed in the lung, heart, and pancreas. Moreover, the suborgan level distribution in the liver and spleen was also restricted. In the liver, the Cy3-siRNA fluorescent signal localized to sinusoids, whereas in the spleen, Cy3-siRNA fluorescent signal was found solely in the red pulp. The addition of the targeting ligands mannose or transferrin to the siRNA/CDP NPs resulted in a mild increase in liver and spleen deposition (Supplementary Fig. S5). Our results are consistent with previously reported data from real-time positron emission tomography studies that showed siRNA/CDP-NPs primarily depositing in liver and kidney [17].

Surface targeting ligands increase mesangial cell uptake of siRNA/CDP-NPs in vitro and alter intraglomerular distribution in vitro

Surface targeting ligands have been demonstrated to improve the cellular internalization efficiencies of nanoparticles [18]. We hypothesized that addition of a targeting ligand to the siRNA/CDP-NPs would result in increased mesangial cell uptake. Therefore, we tested mesangial cell uptake of siRNA/CDP-NPs formulated with two different surface targeting ligands: (1) the sugar mannose and (2) the iron transport protein, transferrin. We chose the mannose targeting ligand because, within the kidney, the expression of the mannose receptor (MR) is restriction to mesangial cells [19,20]. The transferrin targeting ligand was chosen because we have previously demonstrated its ability to enhance intracellular uptake of the siRNA/CDP-NPs in other cell lines in vitro and in vivo [17,21]. However, transferrin receptor is a more general receptor expressed by many cell types, but not highly in the healthy glomerulus [22].

Epifluorescence experiments qualitatively demonstrated similar mesangial cell uptake for the targeted siRNA/CDP-NPs as compared with nontargeted nanoparticles (Fig. 2A). To more carefully quantify the amount of intracellular Cy3-siRNA fluorescence, we employed flow cytometry (Fig. 2B). We observed higher intracellular Cy3-siRNA fluorescence intensities in mouse mesangial cells treated with transferrin-targeted siRNA/CDP-NPs than those treated with untargeted siRNA/CDP-NPs (fluorescence peak mean intensity 47.3 ± 14.1 versus 29.3 ± 0.3; $p < 0.05$). However, transferrin-targeted siRNA/CDP-NP treatment did not result in increased

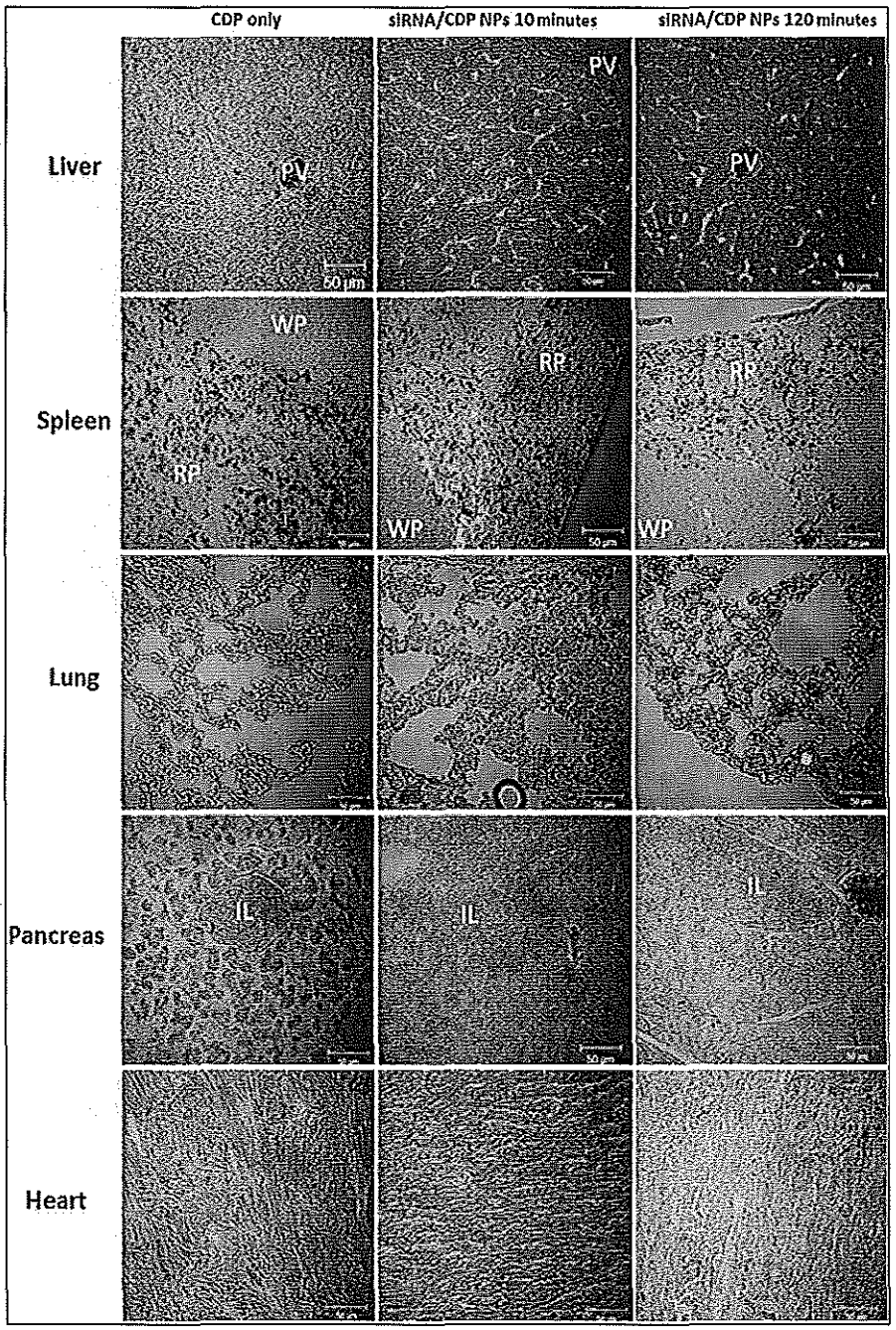

FIG. 4. siRNA/CDP-NPs have a restricted biodistribution outside the kidney. Laser scanning confocal microcopy of tissue sections from the indicated organs taken from mice at 10 and 120 minutes after administration of i.v. doses of Cy3-labeled siRNA/CDP-NPs or CDP polymer. For all images, detector gain was adjusted for maximal dynamic range or until diffuse background autofluorescence was apparent. Global brightness and contrast were adjusted across whole images to improve clarity of images on scale for publication. IL, Islets of Langerhans; PV, portal vein; RP, red pulp; WP, white pulp. Color images available online at www.liebertpub.com/nat

intracellular Cy3-siRNA fluorescence compared with untargeted siRNA/CDP NP treatment in human mesangial cells. Unlike treatment with transferrin-targeted siRNA/CDP NPs, treatment with the mannose-targeted siRNA/CDP-NPs resulted in increased intracellular Cy3-siRNA fluorescence in both mouse and human mesangial cells compared with untargeted siRNA/CDP-NPs (fluorescence peak mean intensity 58.2 ± 2.1 vs. 29.3 ± 0.3; $p < 0.05$) and (90.4 ± 12.3 vs. 43.1 ± 17.0; $p < 0.05$), respectively.

We investigated whether the presence of targeting ligands altered the in vivo intrakidney distributions of the siRNA/CDP-NPs. Fluorescence microcopy on fixed tissue sections (Fig. 4C, D) and quantitative PCR measurements (Fig. 5) were used in these studies. Epifluorescence microscopy imaging was used to examine the distribution and intensity of the Cy3-siRNA fluorescence signal in glomeruli at 10 and 120 minutes after i.v. administration of untargeted siRNA/CDP-NPs and mannose-targeted siRNA/CDP-NPs (Fig. 5A). At 120 minutes after i.v. administration there was a marked attenuation in glomerular fluorescent signal in kidneys from mice treated with untargeted siRNA/CDP-NPs. This attenuation in glomerular signal at 120 minutes post treatment was

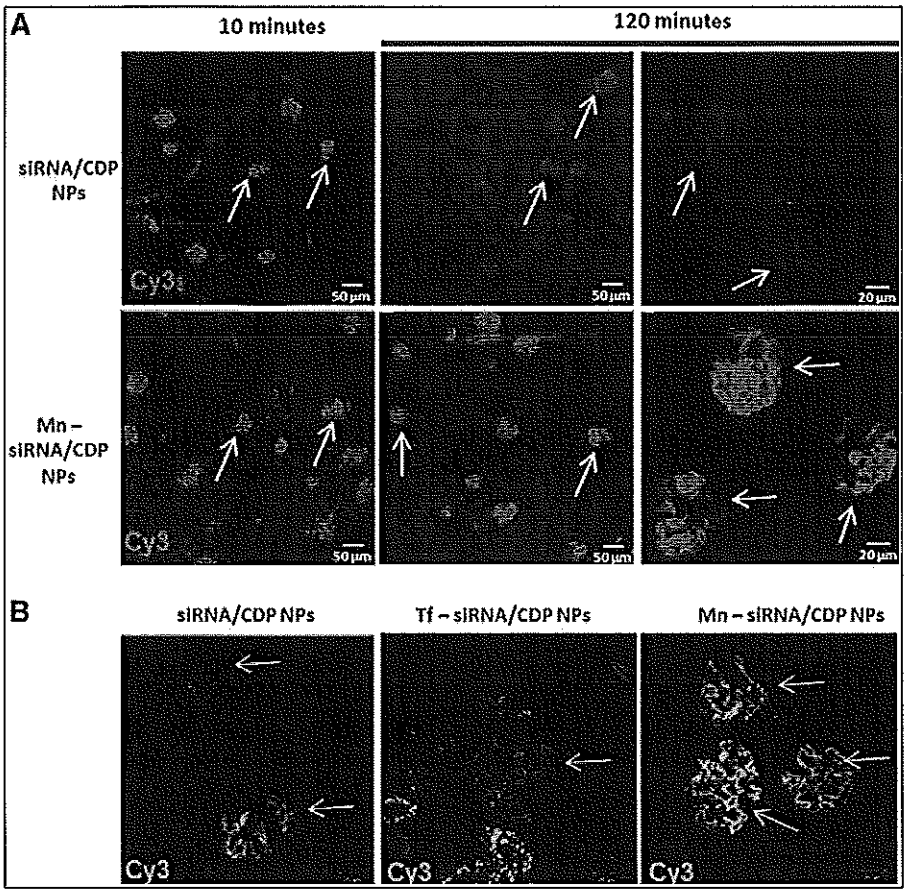

FIG. 5. In vivo uptake of mannose or transferrin targeting siRNA/CDP-NPs. (**A**) Epifluorescence microscopy images of kidney sections from mice that received Cy3-siRNA labeled siRNA/CDP-NPs or siRNA/CDP-NPs with mannose targeting ligands. Arrows point to glomeruli. (**B**) Laser scanning confocal microscopy images of kidney sections from mice 2 hours after i.v. treatment with siRNA/CDP-NPs, Tf-siRNA/CDP-NPs, or Mn-siRNA/CDP-NPs. siRNA/CDP-NPs, untargeted siRNA/CDP-NPs; TF-siRNA/CDP-NPs, transferrin-targeted siRNA/CDP-NPs; Mn-siRNA/CDP-NPs, mannose-targeted siRNA/CDP-NPs. Detector gain and exposure time for all epifluorescence images was fixed for each experiment. Detector gain for all confocal images was adjusted for maximal dynamic range or until diffuse background autofluorescence in proximal tubules was apparent. Images with more visible background are lower in overall fluorescence intensity. Global brightness and contrast were adjusted across whole images to improve clarity of images on scale for publication. Color images available online at www.liebertpub.com/nat

not observed in the kidneys of mice treated with mannose-targeted siRNA/CDP-NPs. These data suggest that mannose targeting of nanoparticles resulted in a longer glomerular residency time for the mannose-targeted siRNA/CDP-NPs. Figure 5B demonstrates that glomerular fluorescence intensity at 120 minutes post treatment in the kidneys of mice treated with transferrin-targeted siRNA/CDP-NPs was similar to untargeted siRNA/CDP-NPs and markedly less than the fluorescence intensity of the mannose-targeted siRNA/CDP-NPs. These data suggest that inclusion of a transferrin targeting ligand did not result in longer glomerular residency times for the siRNA/CDP-NPs.

To more quantitatively assess delivery of targeted siRNA/CDP-NPs to the glomerulus, we used quantitative PCR to interrogate the level of siRNA present in isolated glomeruli from mice receiving i.v. administration of the different siRNA/CDP-NP formulations (Fig. 6). siRNA present in whole RNA extracts from these glomeruli was detected using a custom Taqman real-time PCR probe to detect the presence of the antisense strand of a specific siRNA sequence (siTrace). Glomerular RNA extracts from mice treated with transferrin-targeted siRNA/CDP-NP with a control siRNA sequence (siCON) that is not recognized by the Taqman PCR probe were used as background controls.

We first examined the glomeruli from mice 1 and 3 days after received i.v. doses of free siTrace. At 1 day post dose, siTrace was detectable in RNA extracts from these glomeruli at levels 12-fold above background. At 3 days post dose, siTrace signal in glomerular RNA extracts from this treatment group were not significantly above background. We next examined glomeruli from mice that received i.v. doses of various siRNA/CDP-NP formulations. At 1 day post dose, siTrace signal in glomerular RNA extracts from the nontargeted siRNA/CDP-NP treatment group was found to be 333-fold higher than the siTrace signal detected in the free siTrace treatment group. The amount of siTrace signal in the glomeruli from mice treated with transferrin- or mannose-targeted siRNA/CDP-NPs (356- and 274-fold above background

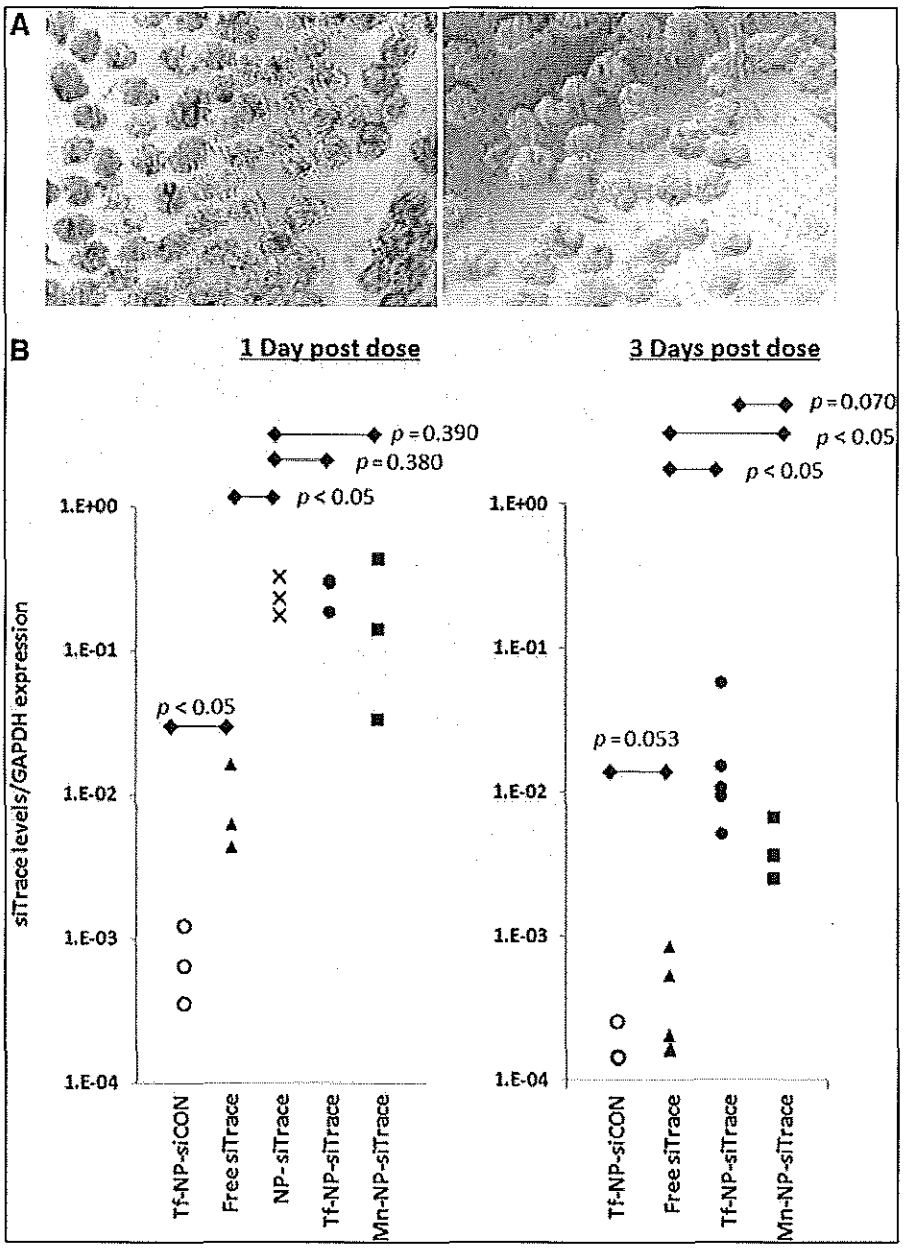

FIG. 6. Quantitative real-time polymerase chain reaction (PCR) detection of siRNA delivery to the glomerulus. **(A)** Light micrographs of two preparations of isolated glomeruli from mouse kidneys. **(B)** Real-time PCR based detection of siTrace in isolated glomeruli from mice 1 and 3 days after i.v. treatment with siRNA/CDP NPs. The Tf-NP-siCON group is a background control (PCR assay does not detect siCON). Tf-NP-siCON, transferrin-targeted siRNA/CDP-NPs with control siRNA (siCON); Tf-NP siTrace, transferrin-targeted siRNA/CDP-NPs with siTrace; Mn-NP siTrace, mannose-targeted siRNA/CDP-NPs with siTrace. GAPDH, glyceraldehyde 3-phosphate dehydrogenase. n = 3 mice (1 day) or n = 5 mice (3 days) per group; p values are from one-tailed t-tests.

respectively) was not significant different from the amount detected in the nontargeted siRNA/CDP-NP group. At 3 days post dose, siTrace signal in the glomeruli from both the transferrin- and mannose-targeted siRNA/CDP-NPs was still significantly higher than siTrace signal detected in the free siRNA treatment group. Although transferrin-targeting lead to a 12-fold increase in total siTrace signal in glomeruli compared with mannose targeting, these results were not significantly different.

siRNA/CDP-NPs silenced gene expression in the mesangium

We next examined the ability of transferrin- and mannose-targeted siRNA/CDP-NPs to silence EGFP expression in the glomeruli of EGFP expressing transgenic mice. We used fluorescence microscopy to examine EGFP fluorescence in kidney sections from each mouse (Fig. 7). A microscopy-based analysis was chosen to facilitate specific analysis of mesangial EGFP expression. We used a blinded, semiquantitative, glomerular fluorescence scoring analysis to determine the level of EGFP expression in the glomerulus. Fluorescence micrographs of 70–72 glomeruli from each mouse were taken and scored as high, intermediate, or low EGFP fluorescence (representative examples of each scoring category are pictured in Supplementary Fig. S6C).

Once scores had been assigned to all imaged glomeruli, the data were unblinded and results from each treatment group were averaged and compared. Kidneys from mice receiving the siRNA/CDP-NPs containing control siRNA (siCON)

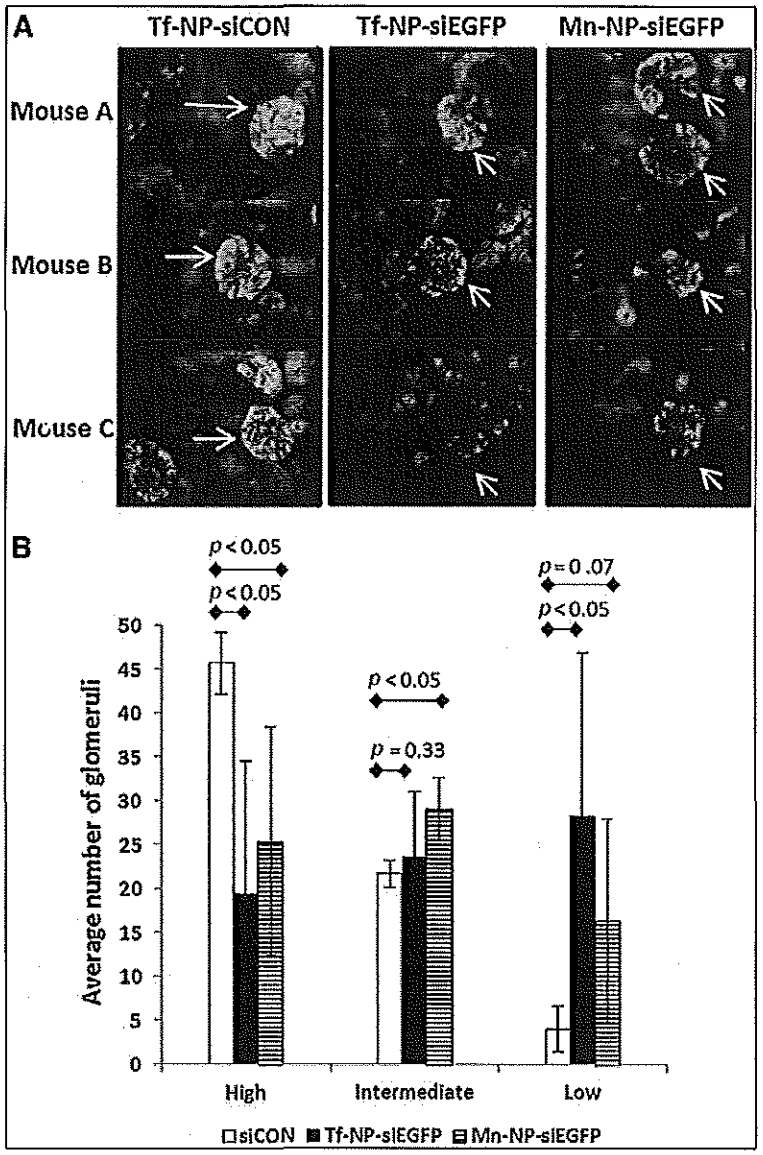

FIG. 7. Evidence for gene silencing in the kidney mesangium following intravenous administration of siRNA/CDP-NPs. (A–B) Analysis of enhanced green fluorescence protein expression (EGFP) in EGFP-expressing transgenic mice following i.v. dosing of siRNA/CDP-NPs with siRNA against EGFP (siEGFP) or control siRNA (siCON). (A) Fluorescence micrographs of median intensity glomeruli from each mouse in the experiment. White arrows point to glomeruli. Tf-NP-siEGFP, transferrin-targeted siRNA/CDP-NPs with siEGFP; Mn-NP-siEGFP, mannose-targeted siRNA/CDP-NPs with siEGFP. (B) Results of semiquantitative scoring analysis of glomerular EGFP fluorescence intensities. For each mouse, 70–72 glomeruli were imaged and scored as high, intermediate, or low EGFP fluorescence (representative examples of each scoring category are pictured in Supplementary Fig. S2). All imaging and scoring were performed blind. The average number of glomeruli from each scoring bin are shown. Error bars are standard deviation; n=3; p values are results of one-tailed t-tests. Color images available online at www.liebertpub.com/nat

were found to have strong expression of EGFP throughout their kidneys. Glomerular EGFP expression was found to be higher than tubules. Within the glomeruli, cells in the glomerular periphery (likely podocytes) had more pronounced EGFP expression than more central glomerular cells (likely mesangial areas) (Supplementary Figure S6A, B). Transferrin- and mannose-targeted siRNA/CDP-NPs containing siEGFP were found to reduce glomerular EGFP expression. EGFP knockdown was most noticeable within the central region of the glomerulus (likely mesangial region). A ~2-fold decrease of glomeruli with high EGFP expression was observed in both transferrin- and mannose-targeted siRNA/CDP-NP treatment groups. A ~6-fold increase in the number of glomeruli with low EGFP expression was observed in the transferrin-targeted siRNA/CDP-NP treated mice, whereas only a ~3-fold non-significant increase was noted in the mannose-targeted siRNA/CDP-NP treatment group. However, a significant increase in the number of glomeruli with intermediate EGFP expression was noted only in the mannose-targeted siRNA/CDP-NP treatment group. Altogether, these data demonstrate gene knockdown in the mesangium following i.v. siRNA/CDP-NP administration.

Discussion

Taken in total, the results from our studies demonstrate the feasibility of siRNA delivery to the mesangium following i.v. administration of siRNA/CDP-NPs. Using confocal microscopy, we demonstrated the presence of Cy3-siRNA in the glomeruli of mice that received i.v. doses of siRNA/CDP-NPs, but not in the glomeruli of mice that received free siRNA. Additionally, we showed that the siRNA/CDP-NPs deposit in the glomerulus as intact nanoparticles as evidenced by the colocalization of Cy3-siRNA and AF350-CDP fluorescence in the glomerulus as well as electron micrographs of nanoparticle sized objects in the glomerular capillary wall.

Colocalization of Cy3-siRNA fluorescence and OX-7 antibody staining for Thy1 antigen confirmed mesangial delivery of the siRNA. Biodistribution studies demonstrated a restricted deposition outside the kidney limited to liver sinusoids (likely in Kupffer cells [23]) and splenic red pulp. Furthermore, we demonstrated that both mouse and human mesangial cells can rapidly internalize the siRNA/CDP-NPs but not free siRNA in vitro and that uptake of the siRNA/CDP-NPs by mesangial cells can be enhanced by surface targeting ligands. Lastly, we showed that i.v. doses of siRNA/CDP-NPs resulted in decreased mesangial expression of EGFP in a EGFP-reporter mouse strain.

To our knowledge, our study is only the second reported example of polymer-nanoparticle mediated siRNA delivery to the mesangium following systemic administration. The first, performed by Shimizu et al. demonstrated that non-targeted 10-nm siRNA/cationic polymer micelles can reach the glomerulus following intraperitoneal administration [10]. Our study builds upon this work by demonstrating the feasibility of using i.v. administration as well as larger ($\sim$70 nm) polymer-based nanoparticles to target the mesangium. Moreover, the siRNA/CDP-NPs used here have previously been demonstrated to deliver function siRNA to patient tumor tissue following i.v. administration in the clinic, and therefore the results presented here have direct translational relevance. We suggest that the siRNA/CDP-NPs could be useful for mesangial delivery of siRNA in humans. Given that the ultrastructure of the glomerulus across mammalian species is nearly identical [24], we speculate that our observations in the mouse kidney would be applicable to delivery to human kidney mesangium. Also, we showed that human mesangial cells more readily uptake the siRNA/CDP-NPs than mouse mesangial cells in vitro.

We investigated if the surface targeting ligands transferrin or mannose could be used to increase mesangial uptake of the siRNA/CDP-NPs. Mannose receptor expression in the kidney is restricted to the mesangium [19,20] and has been demonstrated to facilitate uptake of nanoparticles by macrophages in vivo [25,26]. The transferrin receptor, although up-regulated within the mesangium of patients with IgA nephropathy [27–29], is not highly expressed in the healthy glomerulus, but has been demonstrated to facilitate intracellular uptake of the transferrin-targeted siRNA/CDP-NPs in other cell lines [17,21].

In vitro, the mannose targeting ligand enhanced uptake of the siRNA/CDP-NPs in both mouse and human mesangial cells, whereas the transferrin receptor only enhanced uptake in mouse cells. In vivo, mannose targeting resulted in enhanced glomerular Cy3-siRNA fluoresce intensity 2 hours after i.v. dosing compared with either untargeted or transferrin-targeted siRNA/CDP-NPs. However, these effects were transient as the total amount of siRNA detected in isolated glomeruli by PCR 1 day following i.v. administration was not different among the various siRNA/CDP-NP formulations. Similarly, mannose targeting did not result in any additional benefit in the EGFP knockdown experiment. Surprisingly, the PCR quantification data of siRNA delivery to the glomerulus at 3 days post dose trended higher for the transferrin-siRNA/CDP NP group compared with the mannose-siRNA/CDP NP group (although statistical significance was not achieved). These data suggest that transferrin may be the superior targeting ligand for mesangial targeting. We speculate that mannose targeting may favor trafficking to digestive compartments within the mesangial cell resulting in more rapid degradation of the siRNA/CDP-NPs. Nontargeted, transferrin-targeted, and some fraction of the mannose-targeted siRNA/CDP-NPs may be taken up through alternate pathways (e.g., endocytosis, macropinocytosis, calveolar transport) that are more permissible for endosomal escape and subsequent siRNA delivery to the cytoplasm [18]. Further work to elucidate this mechanism is merited.

Several other non-nanoparticle based strategies of siRNA delivery to the kidney glomerulus have been reported. Hauser et al. have demonstrated that a monovalent Ig-protamine conjugate could successfully deliver siRNA to normal murine podocytes in vivo [11]. Yuan et al., have also shown that subcutaneous administration of cholesterol conjugated phosphorothioate-modified siRNAs targeting 12/15-lipoxegenase reduced kidney damage in diabetic mice [30]. Other reported examples of siRNA delivery to the glomerulus and kidney in general have employed less clinically applicable direct renal artery injections [31]. Nanoparticle mediated delivery of siRNA can be advantageous over these methods due to the highly tunable nature of their pharmacokinetic, biodistribution, and targeting properties compared with free antibodies, phosphorothioate-modified, or other free nucleic acids. Theoretically, these properties of nanoparticles should enable more specific control of targeting and off-target effects.

Our study has several limitations. We confined our experiments to healthy mice. It remains to be determined whether the siRNA/CDP NP system can facilitate gene knockdown in mouse models of kidney disease. However, reports examining nanoparticle delivery to the diseased kidney in animal models [6,9,32–35] suggest that nanoparticles have a higher propensity for glomerular deposition in glomerulonephritic states, likely due to increased vascular permeability and inflammation. Thus, the healthy, rather than the diseased kidney, may provide the more restrictive condition for nanoparticle delivery. Furthermore, many chronic kidney diseases such as diabetic nephropathy display fairly subtle glomerular morphologic changes in early disease, and we speculate that the glomerular nanoparticle targeting criteria may not be significantly altered until advance stage disease. Another limitation of the current study is that we only reported mesangial knockdown of a reporter protein (EGFP) in a transgenic mouse model rather than an endogenous, biologically relevant, mesangial protein. We have performed follow-up experiments that demonstrate knockdown of the endogenous mesangial protein Orai1in mice [36]. Therefore, we believe the knockdown of EGFP reported in this study will be generalizable to other mesangial protein targets.

Acknowledgments

We would like to thank Carol M. Garland (Caltech) for help obtaining electron microscopy images. This work benefited from the use of the Caltech Materials Science Transmission Electron Microscope facility, which is partially supported by the Materials Research Science and Engineering Centers Program of the National Science Foundation under award number DMR-0520565. We thank Han Han for preparing the AF350-CDP and AD-PEG-Mannose, and Chung Hang J. Choi for processing kidney samples for

transmission electron microscope imaging. This work was supported by National Cancer Institute grant CA119347, Sanofi-Aventis, and National Institutes of Health/National Institute of Diabetes and Digestive and Kidney Diseases, DK079968 (to R.M.). Jonathan E. Zuckerman is also supported by the Caltech-University of California Los Angeles (UCLA) Joint Center for Translational Medicine, National Institutes of Health National Institute of General Medical Sciences training grant, GM08042, and the UCLA Medical Scientist Training Program.

Author Disclosure Statement

No financial conflicts exist.

References

1. United States Renal Data System. (2014). 2014 Annual Data Report: Epidemiology of Kidney Disease in the United States. National Institutes of Health, National Institute of Diabetes and Digestive and Kidney Diseases, Bethesda, MD.
2. Davis ME, ZG Chen and DM Shin. (2008). Nanoparticle therapeutics: an emerging treatment modality for cancer. Nat Rev Drug Discov 7:771–782.
3. Castanotto D and JJ Rossi. (2009). The promises and pitfalls of RNA-interference-based therapeutics. Nature 457:426–433.
4. Zuckerman JE and ME Davis. (2013). Targeting therapeutics to the glomerulus with nanoparticles. Adv Chronic Kidney Dis 20:500–507.
5. Choi CHJ, JE Zuckerman, P Webster and ME Davis. (2011). Targeting kidney mesangium by nanoparticles of defined size. Proc Natl Acad Sci (USA) 108:6656–6661.
6. Liao J, K Hayashi, S Horikoshi, H Ushijima, J Kimura and Y Tomino. (2001). Effect of steroid-liposome on immunohistopathology of IgA nephropathy in ddY mice. Nephron 89:194–200.
7. Morimoto K, M Kondo, K Kawahara, H Ushijima, Y Tomino, M Miyajima and J Kimura. (2007). Advances in targeting drug delivery to glomerular mesangial cells by long circulating cationic liposomes for the treatment of glomerulonephritis. Pharm Res 24: 946–54.
8. Asgeirsdóttir SA, JA Kamps, HI Bakker, PJ Zwiers, P Heeringa, K Van Der Weide, H Van Goor, AH Petersen, H Morselt, et al. (2007). Site-specific inhibition of glomerulonephritis progression by targeted delivery of dexamethasone to glomerular endothelium. Mol Pharmacol 72:121–131.
9. Suana AJ, G Tuffin, BM Frey, L Knudsen, C Mu, S Ro and H Marti. (2011). Single application of low-dose mycophenolate mofetil-OX7- Immunoliposomes ameliorates experimental mesangial proliferative glomerulonephritis. Pharmacology 337:411–422.
10. Shimizu H, Y Hori, S Kaname, K Yamada, N Nishiyama, S Matsumoto, K Miyata, M Oba, A Yamada, K Kataoka and T Fujita T. (2010). siRNA-based therapy ameliorates glomerulonephritis. J Am Soc Nephrol 21:622–633.
11. Hauser PV, JW Pippin, C Kaiser, RD Krofft, PT Brinkkoetter, KL Hudkins, D Kerjaschki, J Reiser, CE Alpers and SJ Shankland. (2010). Novel siRNA delivery system to target podocytes in vivo. PloS One 5:e9463.
12. Zuckerman JE, CH Choi, H Han and ME Davis. Polycation-siRNA nanoparticles can disassemble at the kidney glomerular basement membrane.(2012). Proc Natl Acad Sci (USA) 109:3137–3142.
13. Davis ME, JE Zuckerman, CH Choi, D Seligson, A Tolcher, CA Alabi, Y Yen, JD Heidel and A Ribas. (2010). Evidence of RNAi in humans from systemically administered siRNA via targeted nanoparticles. Nature 464:1067–1070.
14. Bartlett DW and ME Davis. (2007). Physicochemical and biological characterization of targeted, nucleic acid-containing nanoparticles. Bioconjug Chem 18:456–468.
15. Novina CD, MF Murray, DM Dykxhoorn, PJ Beresford, J Riess, S-K Lee, RG Collman, J Lieberman, P Shankar and PA Sharp. (2002). siRNA-directed inhibition of HIV-1 infection. Nat Med 8:681–686.
16. Takemoto M, N Asker, H Gerhardt, A Lundkvist, BR Johansson, Y Saito and C Betsholtz. (2002). A new method for large scale isolation of kidney glomeruli from mice. Am J Pathol 161:799–805.
17. Bartlett DW, H Su, IJ Hildebrandt, WA Weber and ME Davis. (2007). Impact of tumor-specific targeting on the biodistribution and efficacy of siRNA nanoparticles measured by multimodality in vivo imaging. Proc Natl Acad Sci (USA) 104:15549–1554.
18. Kamaly N, Z Xiao, PM Valencia, AF Radovic-Moreno and OC Farokhzad. (2012). Targeted polymeric therapeutic nanoparticles: design, development and clinical translation. Chem Soc Rev 41:2971–3010.
19. Linehan S, L Martínez-Pomares, PD Stahl and S Gordon. (1999). Mannose receptor and its putative ligands in normal murine lymphoid and nonlymphoid organs: in situ expression of mannose receptor by selected macrophages, endothelial cells, perivascular microglia, and mesangial cells, but not dendritic cells. J Exp Med 189:1961–1972.
20. Zhang XS, W Brondyk, JT Lydon, BL Thurberg and P Piepenhagen. (2011). Biotherapeutic target or sink: analysis of the macrophage mannose receptor tissue distribution in murine models of lysosomal storage diseases. J Inherit Metab Dis 34:795–809.
21. Bellocq NC, SH Pun, GS Jensen and ME Davis. (2003). Transferrin-containing, cyclodextrin polymer-based particles for tumor-targeted gene delivery. Bioconjug Chem 14:1122–1132.
22. Zhang D, E Meyron-Holtz and T Rouault. (2007). Renal iron metabolism: transferrin iron delivery and the role of iron regulatory proteins. J Am Soc Nephrol 18:401–406.
23. Popielarski SR, S Hu-Lieskovan, SW French, TJ Triche and ME Davis. (2005). A nanoparticle-based model delivery system to guide the rational design of gene delivery to the liver. 2. In vitro and in vivo uptake results. Bioconjug Chem 16:1071–1080.
24. Sraer JD, C Adida, MN Peraldi, E Rondeau and A Kanfer. (1993). Species-specific properties of the glomerular mesangium. J Am Soc Nephrol 3:1342–1350.
25. Kawakami S, A Sato, M Nishikawa, F Yamashita and M Hashida. (2000). Mannose receptor-mediated gene transfer into macrophages using novel mannosylated cationic liposomes. Gene Ther 7:292–299.
26. Wada K, H Arima, T Tsutsumi, Y Chihara, K Hattori, F Hirayama and K Uekama. (2005). Improvement of gene delivery mediated by mannosylated dendrimer/alpha-cyclodextrin conjugates. J Control Release 104:397–413.
27. Haddad E. (2003). Enhanced expression of the CD71 mesangial IgA1 receptor in Berger disease and Henoch-Schonlein nephritis: association between CD71 expression and IgA deposits. J Am Soc Nephrol 14:327–337.
28. Moura IC, MN Centelles, M Arcos-Fajardo, DM Malheiros, JF Collawn, MD Cooper and RC Monteiro. (2001).

Identification of the transferrin receptor as a novel immunoglobulin (Ig)A1 receptor and its enhanced expression on mesangial cells in IgA nephropathy. J Exp Med 194:417–425.
29. Berthelot L, C Papista, TT Maciel, M Biarnes-Pelicot, E Tissandie, PH Wang, H Tamouza, A Jamin, J Bex-Coudrat, et al. (2012). Transglutaminase is essential for IgA nephropathy development acting through IgA receptors. The J Exp Med 209:793–806.
30. Yuan H, L Lanting, Z-G Xu, S-L Li, P Swiderski, S Putta, M Jonnalagadda, M Kato and R Natarajan. (2008). Effects of cholesterol-tagged small interfering RNAs targeting 12/15-lipoxygenase on parameters of diabetic nephropathy in a mouse model of type 1 diabetes. Am J Physiol Renal Physiol 295:F605–F617.
31. Stokman G, Y Qin, Z Rácz, P Hamar and LS Price. (2010). Application of siRNA in targeting protein expression in kidney disease. Adv Drug Deliv Rev 62:1378–1389.
32. Ito K, J Chen, JJ Khodadadian, SV Seshan, C Eaton, X Zhao, ED Vaughan, M Lipkowitz, DP Poppas and D Felsen. (2004). Liposome-mediated transfer of nitric oxide synthase gene improves renal function in ureteral obstruction in rats. Kidney Int 66:1365–1375.
33. Tuffin G, E Waelti, J Huwyler, C Hammer and H-P Marti. (2005). Immunoliposome targeting to mesangial cells a promising strategy for specific drug delivery to the kidney. J Am Soc Nephrol 16:3295–3305.
34. Scindia Y, U Deshmukh, P-R Thimmalapura and H Bagavant. (2008). Anti-alpha8 integrin immunoliposomes in glomeruli of lupus-susceptible mice: a novel system for delivery of therapeutic agents to the renal glomerulus in systemic lupus erythematosus. Arthritis Rheum 58: 3884–3891.
35. Asgeirsdóttir SA, PJ Zwiers, HW Morselt, HE Moorlag, HI Bakker, P Heeringa, JW Kok, CG Kallenberg, G Molema and JM Kamps. (2008). Inhibition of proinflammatory genes in anti-GBM glomerulonephritis by targeted dexamethasone-loaded AbEsel liposomes. Am J Physiol Renal Physiol 294:F554–F561.
36. Wu P, Y Wang, ME Davis, JE Zuckerma, S Chaudhari, M Begg M and R Ma. (2015). Store-operated Ca2+ channel in mesangial cells inhibits matrix protein expression. J Am Soc Nephrol. In press.

Address correspondence to:
Jonathan E. Zuckerman, MD, PhD
Department of Chemical Engineering
California Institute of Technology
1200 East California Boulevard
Pasadena, CA 91125

E-mail: jzuckerman@mednet.ucla.edu

Received for publication August 12, 2014; accepted September 19, 2014.